Progress In Electromagnetics Research, PIER 93, 177–188, 2009

X-BAND MINIATURIZED WIDEBAND BANDPASS FILTER UTILIZING MULTILAYERED MICROSTRIP HAIRPIN RESONATOR

H. Adam, A. Ismail, M. A. Mahdi, M. S. Razalli, A. Alhawari and B. K. Esfeh †

Centre of Excellence for Wireless and Photonic Networks
Department of Computer and Communication Systems Engineering
Faculty of Engineering
Universiti Putra Malaysia
43400 UPM Serdang, Selangor, Malaysia

Abstract—This paper presents a new design of miniaturized wideband bandpass filter using microstrip hairpin in multilayer configuration for X-band application. The strong coupling required for wideband filter is realized by arranging five hairpin resonators in two layers on different dielectric substrates. Since adjacent resonator lines are placed at different levels, there are two possible ways to change coupling strength by varying the overlapping gap between two resonators; vertically and horizontally. In this paper, simulated and measured result for a wideband filter of 4.4 GHz bandwidth at 10.2 GHz center frequency with fifth order Chebyshev response is proposed. The filter is fabricated on 0.254 mm thickness R/T Duroid 6010 and R/T Duroid 5880 with dielectric constant 10.2 and 2.2 respectively using standard photolithography technique. Two filter configurations based on vertical (Type 1) and horizontal (Type 2) coupling variation to optimize the coupling strength are presented and compared. Both configurations produce very small and compact filter size, at $5.0 \times 14.6\,\mathrm{mm}^2$ and $3.2 \times 16.1\,\mathrm{mm}^2$ for the first and second proposed filter type respectively. The measured passband insertion losses for both filters are less than 2.3 dB and the passband return loss is better than −16 dB for filter Type 1 and −13 dB for filter Type 2. Very small and compact filter is achieved where measured results show good agreement with the simulated responses.

Corresponding author: A. Ismail (alyani@eng.upm.edu.my).
† M. S. Razalli is also with School of Computer and Communication Engineering, Universiti Malaysia Perlis, P. O. Box 77, Pejabat Pos Besar, 01007 Kangar, Perlis, Malaysia.

1. INTRODUCTION

Microwave bandpass filter used in many RF/microwave applications is the fundamental component that contributes the overall performance of a communication system. Filters can be designed and fabricated on various materials, preferably being fabricated using standard printed circuit technologies since they can be fabricated easily with low cost.

For filter using microstrip, reducing size is the main challenge of the filter design. Numerous researchers have proposed various configurations for reducing filter size and improving filter performance. Some of the filter configurations are using hairpin resonator [1–4], ring resonator [5–9], step impedance resonator [10], defected ground structure [11, 12], and short circuited stub [13–15].

Among the diverse configurations of microstrip resonator, hairpin resonator is widely used due to its advantages to produce compact filter with simple design procedures. It is able to reduce the size of a filter using folded half-wavelength resonator [16] by more than half of conventional filter size. Wideband bandpass filter with high performance and very small size is required for building modern broadband wireless communication systems such as satellite and mobile communication systems. To achieve this, miniaturization of hairpin filter can be used.

Microstrip hairpin narrowband bandpass filter using via ground holes reported in [17] claimed to have reduced the filter size by 35% from the conventional design by using $\lambda/4$ hairpin resonators, but as the consequence, it needs via ground holes. This configuration takes more time and cost to fabricate. Furthermore, for narrowband design, the gap between two resonators is very small, this may save space and make the filter more compact, but for wideband applications the gap becomes etremely tiny that it is almost impossible to achieve good fabrication using standard photolithography process.

Another reported paper for performance improvement and size reduction of hairpin filter at 2.2 GHz has been reported in [18]. Multilayered stripline hairpin is not only able to reduce the size of the filters, but also gain more bandwidth without resulting in small gap that is difficult to fabricate. Cross coupling between the first and the last resonator provides transmission zeros to improve the stopband characteristics. To provide cross coupling, two of adjacent resonators are placed in the same layer. The filter is designed for 2.2 GHz, where the gap is still tolerable. However for higher frequency range such as X-band, the gap may become much too small to be fabricated precisely. The filter in [18] is fabricated using stripline structure which needs extra ground, which could mean extra cost to fabricate compared with microstrip structure.

Investigation of a compact aperture-coupled multilayer microstrip hairpin resonator bandpass filter reported in [19] claimed 50% reduction from conventional structures, however the size is still bigger compared to [17] and [18] in the same frequency range, and bandwidth is limited due to gap limitation.

For high frequency and wideband application, most of previously reported filter in hairpin resonator strucure exhibit gap issues between two adjacent resonators, whereby this gap is limited by standard fabrication accuracy. Current standard photolithography accuracy is about 0.1 mm. By overlapping adjacent hairpin resonator on different layers [20–24], strong coupling required for wideband filter can be obtained easily without involving small gap that makes it difficult and costly to fabricate.

In this paper, we propose a design of compact hairpin resonator filter in multilayer microstrip configuration, operating in X-band frequency. Without having any gap on the same layer, broader bandwidth can be realized to cover the whole X-band frequency. The simulation and measurement responses of the filter will be described in the next sections.

2. PROPOSED FILTER DESIGN AND SIMULATION

Since the filter is operating at high frequency, the length of hairpin resonators become very short, thus, the "U" turn hairpin type is the optimum shape for designing this filter. The proposed filter design method is simply derived from conventional hairpin resonator filter design. Since each layer has different dielectric constant, ε_r, the hairpin resonator width, w in the bottom layer is different from the upper layer. Synthesis of w/h formula [25] in Equation (1) provides a theoretical background to determine the initial resonator physical dimension depending on the dielectric constant of each layer.

$$\begin{aligned}\frac{w}{h} &= \frac{2}{\pi}\Big\{(B-1)-\ln(2B-1)\\&\quad+\frac{\varepsilon_r-1}{2\varepsilon_r}\left[\ln(B-1)+0.39-\frac{0.61}{\varepsilon_r}\right]\Big\}\quad\text{with } B=\frac{60\pi^2}{Z_0\sqrt{\varepsilon_r}}.\end{aligned}\tag{1}$$

With $50\,\Omega$ resonator line impedance choosen, the upper layer resonator width should be bigger than the bottom layer width simply because the upper layer resonator has longer distance to the ground. In order to make the resonator width at bottom layer close to the width at upper layer, the dielectric constant for bottom layer should be lower than the dielectric constant in upper layer. For single layer filter, the resonator width can be calculated directly from Equation (1), but for multilayer filter that has different dielectric constant for each layer, the resonator width and the resonator length should be optimized using an electromagnetic (EM) simulator [27], with the help of Equation (1) as a starting point

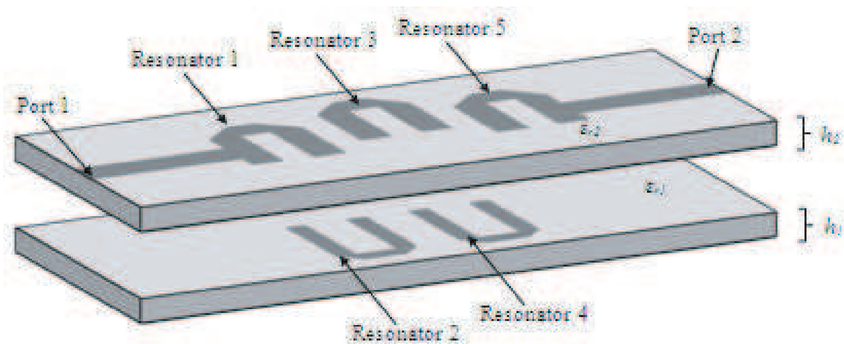

Figure 1. Three dimensional view of the proposed filter.

Figure 1 shows the general multilayer hairpin filter structure. In order to cover the whole X-band frequency range, the filter should have 44% bandwidth at center frequency of 10.2 GHz. A fifth-order 0.1 dB ripple Chebyshev response [14] can satisfy these requirements. Using Table 4.05 of [26], the prototype parameters for $n = 5$ can be obtained. For this design, the prototype parameters obtained are as follows:

$$g_0 = g_6 = 1,$$
$$g_1 = g_5 = 1.1468,$$
$$g_2 = g_4 = 1.3712,$$
$$g_3 = 1.9750$$

From lowpass prototype parameters (g_n) [26], the bandpass design parameters, such as external quality factor, Q_e and coupling coefficient, $M_{i,i+1}$ between resonator i and resonator $i+1$ can be calculated by [14]:

$$Q_{e1} = \frac{f_0 g_1}{\Delta BW}, \quad Q_{en} = \frac{f_0 g_n g_{n+1}}{\Delta BW} \tag{2}$$

$$M_{i,i+1} = \frac{\Delta BW}{f_0 \sqrt{g_i g_{i+1}}} \text{ for } i = 1 \text{ to } n-1 \tag{3}$$

where n is the filter order or number of resonator and ΔBW is the desired bandwidh.

In EM simulator, the external quality factor and coupling coefficient can be computed directly by using [25]:

$$Q_e = \frac{f_0}{BW_{3\,\mathrm{dB}}} \tag{4}$$

$$M_{i,i+1} = \frac{f_2^2 - f_1^2}{f_2^2 + f_1^2} \tag{5}$$

where $BW_{3\,\mathrm{dB}}$ is the 3 dB bandwidth obtained by EM simulator and f_1 and f_2 are frequency peak generated by electromagnetic interaction between the resonators.

The external quality factor and coupling coefficient obtained from EM simulator in Equations (4) and (5) should be matched with the external quality factor and coupling coefficient obtained from lowpass prototype parameters in Equations (2) and (3) respectively. They can be optimized by varying feedline position from the first or the last resonator and varying the gap between two adjacent resonators.

Using Equations (2) and (3), the external quality factor and coupling coeficient matrix, M can be obtained as follows:

$$\begin{aligned} Q_{e1} &= Q_{e5} = 2.66, \\ M &= \begin{bmatrix} 0 & 0.344 & 0 & 0 & 0 \\ 0.344 & 0 & 0.262 & 0 & 0 \\ 0 & 0.262 & 0 & 0.262 & 0 \\ 0 & 0 & 0.262 & 0 & 0.344 \\ 0 & 0 & 0 & 0.344 & 0 \end{bmatrix} \end{aligned}$$

Since this filter is implemented in two layer structure, adjacent resonator lines are placed on different levels, so there are two possible ways to vary the overlapping gap between two adjacent resonators. Figure 2 shows the variation of coupling coefficient for two types of filter. Firstly, the resonator position can be changed by the vertical center of resonator line position on the bottom layer, inline with the upper layer as shown in Figure 2(a). Secondly, the resonator position can be adjusted horizontally as shown in Figure 2(b), where both resonators on the bottom and upper layer are horizontally alligned. The configuration of filter Type 1 in Figure 2(a) will theoretically produce shorter length compared to the filter Type 2 in Figure 2(b). On the other hand, filter Type 2 will produce smaller overall filter width compared to filter Type 1.

It can be seen that for filter Type 1, the resonator is moving vertically to change the coupling strength, whereas for filter Type 2 the resonator is moving horizontally. As expected, the $M_{i,i+1}$

value is increased corresponding to overlapping gap increased. From Figure 2(a), the overlapping gaps for filter Type 1 that satisfy $M_{12} = M_{45}$ and M_{34} value from Equation (3) are 1.5 mm and 0.8 mm respectively, and from Figure 2(b) the overlapping gaps for filter Type 2 are 0.3 mm and 0.15 mm. Figure 3 shows the external quality factor, by finding the best feed position from the first or last resonator. From Figure 3, the feed position that satisfies $Q_{e1} = Q_{e5}$ value from Equation (2) is 1.1 mm. The dimensions for both filter types are shown in Figure 4.

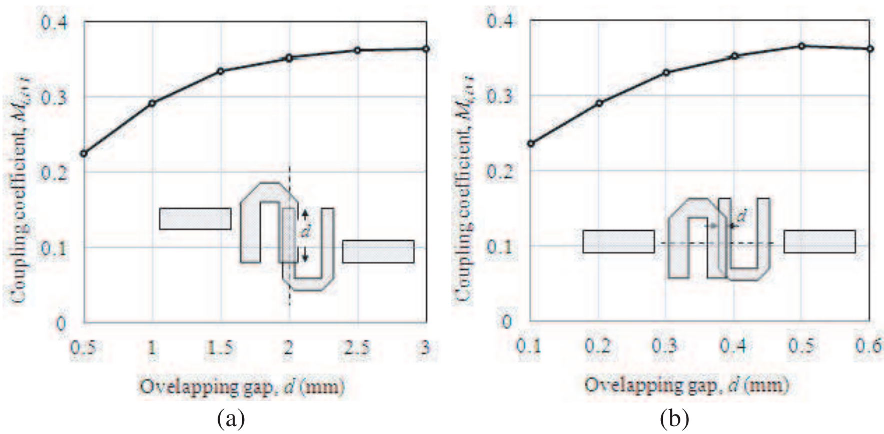

Figure 2. Variation of coupling coefficient due to overlapping gap between two resonators on different substrate layer. (a) Filter Type 1. (b) Filter Type 2.

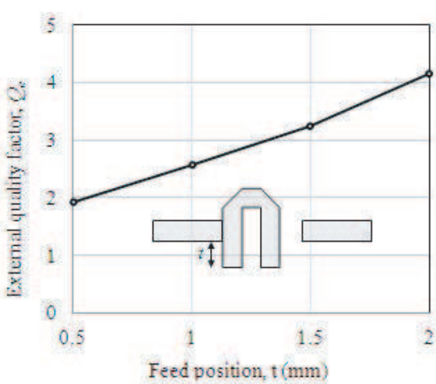

Figure 3. Feed position vs. external quality factor.

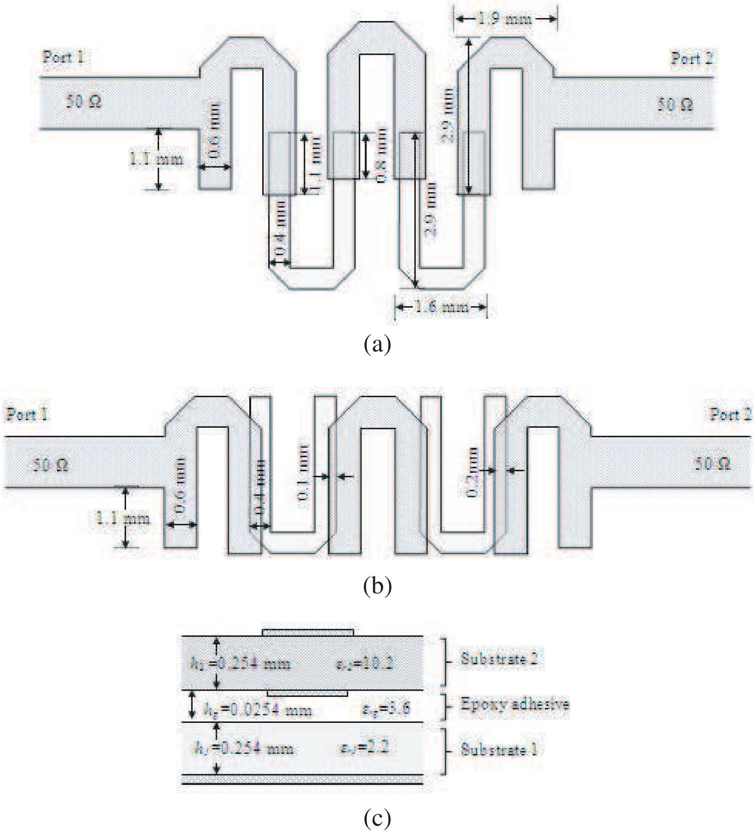

Figure 4. Proposed filter layout and physical dimension. (a) Filter Type 1. (b) Filter Type 2. (c) Cross section view.

3. SIMULATION AND MEASUREMENT RESULT

Using the optimized physical dimensions in Figure 4, the filter circuits are simulated using an EM simulator [27]. The designed filter circuits are then fabricated using standard photolithography process. The photographs of the fabricated filters are shown in Figure 5.

The photographs of fabricated filters shown in Figure 5, exhibit a miniaturized filter size. The overall dimension are $5.0 \times 14.6\,\mathrm{mm}^2$ and $3.2 \times 16.1\,\mathrm{mm}^2$ for filter Type 1 and Type 2 respectively. The miniaturized filter is demonstrated at X-band, which is at higher frequency than the reported filter in [17] to [19]. Even if our proposed filter is to be made to operate in the same frequency band as in [17–19], our filter configuration will offer smaller size compared to microstrip filters in [17] and [19], and comparable with the stripline filter in [18], since from 10.2 GHz, downstreaming to 2.2 GHz, the hairpin resonator length will just be increased by about 10 mm only.

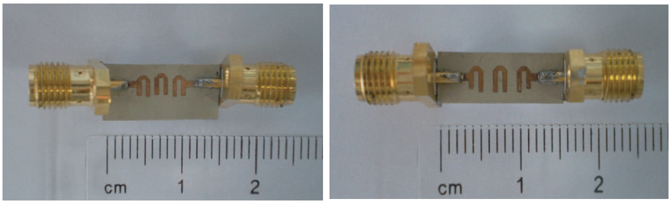

(a) (b)

Figure 5. Photograph of the fabricated filters. (a) Filter Type 1. (b) Filter Type 2.

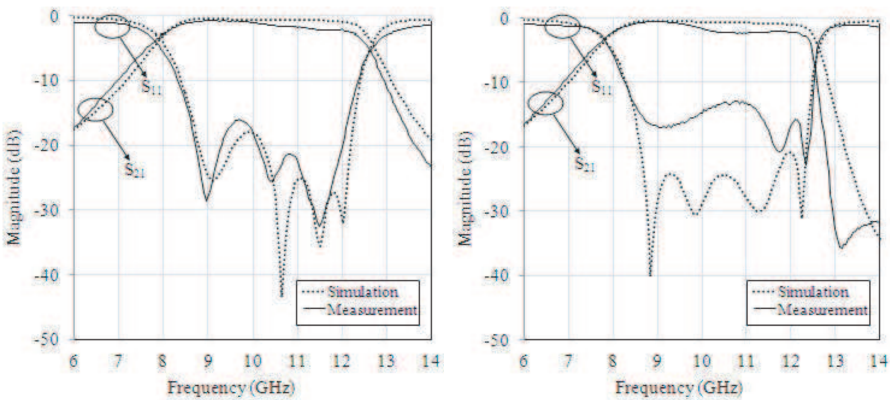

(a) (b)

Figure 6. Simulated and measured responses. (a) Filter type 1. (b) Filter type 2.

The measurements for the fabricated filter are performed by using Agilent E8362B PNA Network Analyzer. Figure 6 shows the simulated and measured filter responses for both filter types. As shown in Figure 6, each filter has slightly different responses. Filter Type 1 has symmetrical balance slope sharpness between low and high frequency, but the filter Type 2 shows asymetrical response. The slope in high frequency is sharper than in the low frequency. The simulated passband return loss for the filter Type 1 is better than −17.8 dB, and for filter Type 2, it is better than −20.8 dB. The simulated passband insertion loss is about 0.5 dB, resulting from the conductor and substrate losses which are included in simulation. However the measured insertion loss is about 2.3 dB, meaning that the losses are contributed not only by material losses, but also connectors and adhesive being used. The measured passband return loss is also slightly different with the simulated results. For filter Type 1, the measured passband return loss is better than −16 dB and for filter Type 2, it is better than −13 dB. Nonetheless, good agreement between the simulated and measured filter performance is shown.

All of the losses are contributed by the fabrication tolerance, material loss and SMA connectors, but mainly due to the epoxy adhesive loss that is used to join the two substrates. However this loss is still tolerable since the measured passband return loss is still better than −10 dB, insertion loss less than 3 dB, and the measured center frequency agrees well with the simulation.

Figure 7 shows the simulated and measured group delay for both filters. For filter Type 1, the measured group delay in the passband varies between 0.39 ns to 0.52 ns, giving only small variation of 1.3 ns. For filter Type 2, the measured group delay in the passband, varies between 0.43 ns to 0.82 ns, giving only 0.39 ns variation which is stable across the passband. Comparing the group delay performance for these

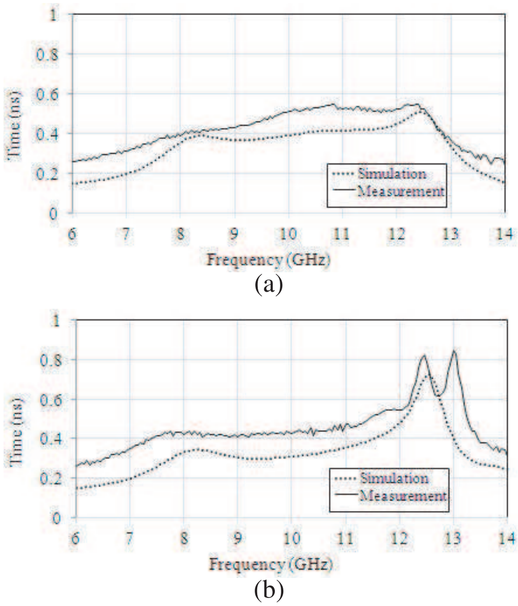

Figure 7. Simulated and measured group delay. (a) Filter Type 1. (b) Filter Type 2.

filters to the stripline filter proposed in [18], the filters proposed here have better group delay variation.

4. CONCLUSIONS

A new design of multilayer hairpin wideband filter in two-layer configurations has been presented. Since the strong coupling needed for wideband filter can be easily obtained by overlapping two hairpin resonators, the filter can produce wider bandwidth. Another benefit that this filter offer is the freedom to choose high dielectric constant substrate without tight concern on resulting very small gap that therefore be difficult and costly to be fabricated.

For this type of filter, there are two possible ways to change the coupling strength, by moving the resonator position vertically or horizontally. Both have different benefit, one can reduce the filter length, and obtain symetrical response, while the other can reduce filter width, giving sharper rejection in high frequency.

In the simulation, adhesive layer for joining the two substrates is added as an extra layer between the substrates. However, the measured passband insertion and return loss are higher than the simulated responses. The losses are mainly resulted from the adhesive layer itself since it is being applied manually on the substrate. With more advance way of joining the substrate, the loss should be reduced. However this loss is still tolerable since the insertion loss is better than 3 dB and the measured passband return loss is better than −10 dB. The filter shows good potential for broadband communication, and can easily be fabricated on the commercial PCB substrate using cheap standard photolithography process.

REFERENCES

1. Sagawa, M., K. Takahasi, and M. Makimoto, "Miniaturized hairpin resonator filters and their application to receiver front-end MIC's," *IEEE Trans. Microwave Theory Tech.*, Vol. 37, No. 10, 1991–1997, 1989.
2. Hong, J. S. and M. J. Lancaster, "Cross-coupled microstrip hairpin-resonator filters," *IEEE Trans. Microwave Theory Tech.*, Vol. 46, 118–122, Jan. 1998.
3. Yoon, H. K., Y. J. Yoonjoo, H. Park, and S. Ye, "Hairpin line half wave parallel coupled line narrowband band pass filters using high temperature superconducting thin films," *IEEE Trans. Applied Superconductivity*, Vol. 9, 901–3904, Jun. 1999.

4. Kikkert, C. J., "Designing low cost wideband microstrip bandpass filters," *Tencon 2005 IEEE Region 10*, 1–6, Nov. 2005.
5. Fan, J. W., C. H. Liang, and X. W. Dai, "Design of cross-coupled dual-band filter with equal-length split-ring resonators," *Progress In Electromagnetics Research*, PIER 75, 285–293, 2007.
6. Wang, Y. X., B. Z. Wang, and J. P. Wang, "A compact square loop dual-mode bandpass filter with wide stop-band," *Progress In Electromagnetics Research*, PIER 77, 67–73, 2007.
7. Zhao, L. P., X. Zhai, B. Wu, T. Su, W. Xue, and C. H. Liang, "Novel design of dual-mode bandpass filter using rectangle structure," *Progress In Electromagnetics Research B*, Vol. 3, 131–141, 2008.
8. Lin, W. J., C. S. Chang, J. Y. Li, D. B. Lin, L. S. Chen, and M. P. Houng, "Improved compact broadband bandpass filter using branch stubs co-via structure with wide stopband characteristic," *Progress In Electromagnetics Research C*, Vol. 5, 45–55, 2008.
9. Lai, X., Q. Li, P. Y. Qin, B. Wu, and C. H. Liang, "A novel wideband bandpass filter based on complementary split-ring resonator," *Progress In Electromagnetics Research C*, Vol. 1, 177–184, 2008.
10. Zhang, J., J. Z. Gu, B. Cui, and X. W. Sun, "Compact and harmonic suppression open-loop resonator bandpass filter with tri-section sir," *Progress In Electromagnetics Research*, PIER 69, 93–100, 2007.
11. Weng, L. H., Y. C. Guo, X. W. Shi, and X. Q. Chen, "An overview on defected ground structure," *Progress In Electromagnetics Research B*, Vol. 7, 173–189, 2008.
12. Boutejdar, A., A. Elsherbini, A. Balalem, J. Machac, and A. Omar, "Design of new DGS hairpin microstrip bandpass filter using coupling matrix method," *PIERS Proceedings*, 261–265, Prague, Czech Republic, August 27–30, 2007.
13. Razalli, M. S., A. Ismail, M. A. Mahdi, and M. N. Hamidon, "Novel compact microstrip ultra-wideband filter utilizing short-circuited stubs with less vias," *Progress In Electromagnetics Research*, PIER 88, 91–104, 2008.
14. Shobeyri, M. and M. H. Vadjed-Samiei, "Compact ultra-wideband bandpass filter with defected ground structure," *Progress In Electromagnetics Research Letters*, Vol. 4, 25–31, 2008.
15. Wei, F., L. Chen, X.-W. Shi, X. H. Wang, and Q. Huang, "Compact UWB bandpass filter with notched band," *Progress In Electromagnetics Research C*, Vol. 4, 121–128, 2008.

16. Cohn, S. B., "Parallel-coupled transmission-line-resonator filters," *IRE Transactions on Microwave Theory and Techniques*, Vol. 6, No. 4, 223–231, April 1958.
17. Hasan, A. and A. E. Nadeem, "Novel microstrip hairpinline narrowband bandpass filter using via ground holes," *Progress In Electromagnetics Research*, PIER 78, 393–419, 2008.
18. Mu, Y., Z. Ma, and D. Xu, "Multilayered stripline interdigital-hairpin bandpass filters with small-size and improved stop-band characteristics," *Asia-Pacific Microwave Conference 2005, Suzhou, China*, Dec. 2005.
19. Djaiz, A. and T. A. Denidni, "Investigation of a compact aperture-coupled multilayer bandpass filter for wireless systems," *Radio and Wireless Conference, 2004 IEEE*, Sept. 2004.
20. Schwab, W. and W. Menzel, "Compact bandpass filters with improved stop-band characteristics using planar multilayer structures," *IEEE MTT-S, Digest*, 1207–1210, 1992.
21. Chang, H. C., C. C. Yeh, W. C. Ku, and K. C. Tao, "A multilayer bandpass filter integrated into RF module board," *IEEE MTT-S, Digest*, 619–622, 1996.
22. Cho, C. and K. C. Gupta, "Design methodology for multilayer coupled line filters," *IEEE MTT-S, Digest*, 785–788, 1997.
23. Cho, C. and K. C. Gupta, "Design of end-coupled band-pass filters in multilayer microstrip configurations," *IEEE MTT-S, Digest*, 711–714, 1999.
24. Matsanaga, M., M. Katayama, and K. Yasumoto, "Coupled mode analysis of line parameters of coupled microstrip lines," *Progress In Electromagnetic Research*, PIER 24, 1–17, 1999.
25. Hong, J. S. and M. J. Lancaster, *Microstrip Filters for RF/Microwave Applications*, Wiley, New York, 2001.
26. Matheai, G. L., L. Young, and E. M. T. Jones, *Microwave Filters, Impedance-Matching Networks, and Coupling Structures*, Artech House, Dedham, 1980.
27. CST Microwave Studio Version 2006B.